References

BREMERMANN, H. (1985). *Distributions, Complex Variables, and Fourier Transforms.* Reading, MA: Addison-Wesley.

COCHRAN, W. (1955). *Acta Cryst.* **8**, 473-478.

GRADSHTEYN, I. S. & RYZHIK, I. M. (1980). *Table of Integrals, Series and Products.* New York: Academic Press.

International Tables for X-ray Crystallography (1965). Vol. I. Birmingham: Kynoch Press.

SHMUELI, U., RABINOVICH, S. & WEISS, G. H. (1989*a*). *Acta Cryst.* **A45**, 361-367.

SHMUELI, U., RABINOVICH, S. & WEISS, G. H. (1989*b*). *Acta Cryst.* **A45**, 367-371.

SHMUELI, U. & WEISS, G. H. (1985). *Acta Cryst.* **A41**, 401-408.

WATSON, G. N. (1922). *A Treatise on the Theory of Bessel Functions.* Cambridge Univ. Press.

Acta Cryst. (1992). A**48**, 423-430

Magnetic *Pendellösung* Effects in Neutron Scattering by Perfect Magnetic Crystals

BY V. V. KVARDAKOV AND V. A. SOMENKOV

I. V. Kurchatov Institute of Atomic Energy, Moscow 123182, *Russia*

(*Received* 18 *December* 1990; *accepted* 6 *December* 1991)

Abstract

Pendellösung effects in magnetic neutron scattering by thin (thickness of the order of the extinction length) crystals of weak ferromagnets $FeBO_3$ and α-Fe_2O_3 were investigated. Dynamical oscillations in the scattering intensity dependences on the crystal's effective thickness, temperature and magnetic field orientation have been found. The influence of irregularities in the magnetic structure related to domains, a magnetic phase transition and magnetoelastic oscillations on the *Pendellösung* oscillation amplitude has been established. The oscillation amplitude and the scattering intensity dependence on the structure-factor magnitude have been used to obtain information on small deformations from perfection of the crystalline and magnetic structures, which are difficult to detect by other methods.

Introduction

In the case of diffraction by a perfect crystal, the wave field is determined by the dynamical interaction between the transmitted and scattered waves (Zachariasen, 1945; Laue, 1960). This results in a number of dynamical effects, one of which is the *Pendellösung* effect, *i.e.* an oscillating dependence of the scattered intensity in Laue geometry on the ratio of the crystal thickness to the extinction length. The dynamical oscillations were studied in detail in X-ray scattering (Kato & Lang, 1959; Utemisov, Somenkova, Somenkov & Shilstein, 1980) and in nuclear neutron scattering (Sippel, Kleinstück & Schulze, 1965; Shull, 1968; Somenkov, Shilstein, Belova & Utemisov, 1978). The theoretical aspects of neutron scattering by perfect magnetically ordered crystals were treated in a number of papers (Stassis & Oberteuffer, 1974; Sivardière, 1975; Gukasov & Ruban, 1975; Schmidt & Deimel, 1976; Belyakov & Bokun, 1975, 1976; Mendiratta & Blume, 1976; Baryshevskii, 1976; Guigay & Schlenker, 1978). However, *Pendellösung* oscillations were observed in the magnetic neutron scattering case only recently (Baruchel, Guigay, Mazure-Espejo, Schlenker & Schweizer, 1982; Kvardakov, Somenkov & Shilstein, 1988; Zelepukhin, Kvardakov, Somenkov & Shilstein, 1989) owing to the small number of perfect magnetically ordered crystals.

Baruchel *et al.* (1982) used the anisotropy of the defect distribution in incompletely perfect yttrium iron garnet crystals. The analyzed reflection had an orientation of the scattering vector such that the effect of defects on the diffraction was minimal. As a result, a peak corresponding to one of the dynamical oscillations was found in the dependence of the mixed (nuclear–magnetic) scattering intensity of polarized neutrons on the wavelength.

Kvardakov, Somenkov & Shilstein (1988) and Zelepukhin, Kvardakov, Somenkov & Shilstein (1989) reported on the *Pendellösung*-effect observation in pure magnetic neutron scattering by using the inclination method. The method was proposed earlier by Somenkov *et al.* (1978) for the case of nuclear neutron scattering and later it was used for *Pendellösung*-effect investigation in X-ray (Utemisov *et al.*, 1980) and synchrotron-radiation (Belova & Kabannik, 1985) scattering, for precise determination of structure factors (Saka & Kato, 1986) and for the study of extinction parameters connected with microdefects (Voronkov, Piskunov, Chukhovskii & Maksimov, 1987).

In works of Kvardakov, Somenkov & Shilstein (1988) and Zelepukhin *et al.* (1989), thin (of the order of the extinction length) crystals of weak ferromagnets iron borate $FeBO_3$ and hematite α-Fe_2O_3 were

0108-7673/92/040423-08$06.00

used. The crystal thicknesses were increased by a factor of 6–7 by rotating the crystals around the normal to the reflecting plane. As a result, several distinct dynamical oscillations were found in the dependences of the magnetic, nuclear and mixed neutron scattering intensities on the effective crystal thickness.

In magnetic neutron scattering, a number of dynamical effects should be observed which do not occur in X-ray and nuclear neutron diffraction. Thus, since the extinction length is determined by the amplitude of scattering by a unit cell, one should expect the existence of dynamical oscillations in the diffracted intensity dependences on different parameters determining the scattering amplitude. So the magnetic neutron scattering intensity should oscillate while changing the sublattice magnetic moment orientation and while varying the sample temperature (Shilstein & Somenkov, 1975; Kvardakov, Somenkov & Shilstein, 1988).

The present paper is devoted to a detailed study of the *Pendellösung* effect on thickness, temperature and orientation dependences of the intensities of magnetic neutron scattering by weak ferromagnet crystals, as well as to the analysis of the effect of magnetic structure irregularities assigned to the domains, magnetic phase transition and magnetoelastic oscillations on the *Pendellösung* oscillation amplitude.

Theory

According to theory (Belyakov & Bokun, 1975), the expression for the integrated reflectivity in magnetic Laue scattering of nonpolarized neutrons in an antiferromagnet is analogous to the formula known for nuclear neutron scattering in paramagnetic crystals,

$$R = \frac{\lambda^2 |F|}{2V \sin 2\theta_b} \left(\frac{\cos \gamma_h}{\cos \gamma_0}\right)^{1/2} \int_0^{2\pi t/t_{ext}} J_0(x)\, dx \qquad (1)$$

where

$$t_{ext} = \pi V [(\cos \gamma_0)(\cos \gamma_h)]^{1/2} / |F| \lambda. \qquad (2)$$

Here, t is the crystal thickness; t_{ext} is the extinction length; λ is the wavelength; V is the unit-cell volume; F is the scattering structure factor; $J_0(x)$ is the Bessel function; θ_b is the Bragg angle; γ_0 and γ_h are the angles between the normal to the crystal surface and the incident and scattered wave directions. By using Δ to denote the angle between the normals to the reflecting plane and the crystal surface and α to denote that of the crystal axis inclination around the normal to the reflecting plane, one can obtain

$$\begin{aligned} \cos(\gamma_0) &= (\sin\theta_b)(\sin\Delta) \\ &\quad + (\cos\theta_b)(\cos\Delta)(\cos\alpha) \\ \cos(\gamma_h) &= -(\sin\theta_b)(\sin\Delta) \\ &\quad + (\cos\theta_b)(\cos\Delta)(\cos\alpha). \end{aligned} \qquad (3)$$

The structure factor has the form

$$F = \sum_{i=1}^{N} a_i \exp(2\pi i \boldsymbol{\tau} \cdot \mathbf{r}_i) \exp(-W_i) \qquad (4)$$

where $\boldsymbol{\tau}$ is the scattering vector, W is the Debye-Waller factor, $\mathbf{r}_i$ is the ith-atom coordinate in the unit cell, a_i is the scattering amplitude of this atom, which, in the case of coherent magnetic scattering of unpolarized neutrons in a collinear antiferromagnet, may be written in the form

$$a = r_0 \mu (\sin\psi) S(T) f(\tau). \qquad (5)$$

Here, r_0 is the classical electron radius, μ is the neutron magnetic moment in nuclear magnetons, ψ is the angle between the normal to the reflecting plane and the vector $\mathbf{L}$ ($\mathbf{L} = \mathbf{M}_1 - \mathbf{M}_2$, where $\mathbf{M}_i$ are the sublattice magnetizations), $S(T)$ is the mean statistical projection (which may be positive or negative) of the atom spin, expressed in units of $\hbar$, on the $\mathbf{L}$ axis, T is the crystal temperature, f is the form factor.

It follows from (1) that the R value is an oscillating function of the integration upper bound (Fig. 1). Taking into account (2)–(5), it is possible to conclude that the intensity of magnetic Laue neutron scattering should oscillate while changing:

(1) the effective thickness of the crystals (*e.g.* through the sample inclination);
(2) the wavelength λ;
(3) the temperature T;
(4) the $\mathbf{L}$ orientation (by changing the ψ angle).

The first and second types of oscillations are common in X-ray and nuclear neutron diffraction, while the observation of the third is difficult owing to the weak Debye-Waller-factor dependence on T. The fourth can be observed only for magnetic neutron diffraction.

Samples and experimental set-up

In the experiments, use was made of the 'easy-plane' weak ferromagnets iron borate $FeBO_3$ and hematite α-Fe_2O_3 crystals. In these crystals, the value of the ferromagnetic moment $\mathbf{M}$ ($\mathbf{M} = \mathbf{M}_1 + \mathbf{M}_2$) is much lower than $|\mathbf{L}|$ ($M/L < 2\%$) (Diehl, Jantz, Nolang & Wettling, 1984). Therefore, the effect of the $\mathbf{M}$ vector on the diffraction was not taken into account. The samples were placed in a saturating magnetic field

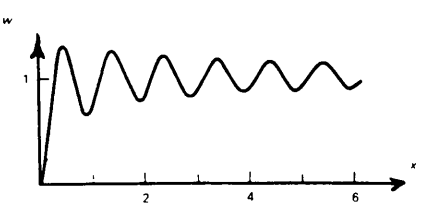

Fig. 1. The plot of the function $W(x) = \int_0^{2\pi x} J_0(u)\, du$.

($H \simeq 4$ kA m^{-1}) in the direction of the easy plane. In this case, **M** was oriented parallel to the field direction, while **L** was perpendicular to it. To change the **L** orientation, the magnetic field was rotated in the easy plane where the magnetic anisotropy is negligible (less than 80 A m^{-1}).

The experiments were carried out on the single-crystal diffractometer MOND at the IR-8 research reactor of the I. V. Kurchatov Institute of Atomic Energy in Moscow. Neutrons with wavelength $\lambda =$ 2.4 Å were used. For monochromatization, reflection by two crystals [the double monochromator (Entin, Glazkov & Moryakov, 1976)] of pyrolytic graphite with mosaic spread of ~20′ was used. A graphite filter diminished the flux of neutrons with wavelength $\lambda/2$ down to the level of approximately 2%.

The iron borate crystals used in this work were grown at the Physical Institute of the Czechoslovak Academy of Sciences in Prague, those of hematite at Simferopol State University (Crimea). The samples were plates with a surface parallel to the easy plane. The crystal thickness was determined by X-ray absorption. The crystal thickness and dimensions were: 100 μm, 6×6 mm ($FeBO_3$ crystal no. 1); 75 μm, 5×9 mm ($FeBO_3$ crystal no. 2); 14 μm, 5×3 mm (α-Fe_2O_3 crystal). In different experiments, the beam diameter varied from 1 to 3 mm. The thickness inhomogeneity of the sample region illuminated by the beam amounted to ~7% for $FeBO_3$ and ~14% for α-Fe_2O_3.

Results

(1) *Intensity oscillations in crystal inclination*

Using (1)–(3), it is possible to obtain the scattering intensity dependence on the inclination angle,

$$I(\alpha) \sim \left[\frac{|\cos\alpha - (\tan\Delta)(\tan\theta_b)|}{|\cos\alpha + (\tan\Delta)(\tan\theta_b)|}\right]^{1/2} \times \int_0^{2\pi(t/t_{ext})_{\alpha=0}\eta(\alpha)} J_0(x)\,dx, \quad (6)$$

where

$$\eta(\alpha) = \left(\frac{|1 - [(\tan\Delta)(\tan\theta_b)]^2|}{|\cos^2\alpha - (\tan^2\Delta)(\tan^2\theta_b)|}\right)^{1/2} \quad (7)$$

determines the increase of the crystal optical thickness in its inclination.

The experiments were performed at room temperature. The magnetic field direction corresponded to $\psi = 90°$, therefore the structure factor had the maximum value, as compared with the other directions. The dependence of the intensity of the magnetic neutron scattering by the $FeBO_3$ crystals (the 100 reflection, $\Delta = 15.5°$, $\theta_b = 18.1°$) on the α value was measured.

As is seen from the results of experiments performed on the $FeBO_3$ crystal no. 1 (Fig. 2), the scattering intensity oscillates with the sample inclination. The nodal and antinodal positions correspond to those on a theoretical curve, where the thickness inhomogeneity is taken into account by averaging the $I_t(\alpha)$ curves calculated for different crystal regions:

$$I(\alpha) \sim \int_{t_{min}}^{t_{max}} I_t(\alpha)\rho(t)\,dt, \quad (8)$$

where $\rho(t)$ is the area of the crystal region with thickness t. The dynamical oscillations were also observed in nuclear neutron scattering and in scattering by the α-Fe_2O_3 crystal.

Fig. 3 shows the intensity of neutron scattering by the iron borate crystal no. 2 *vs* the $\eta(\alpha)$ value. Neglecting the influence of the monotonic function on the nodes and antinodes, one can write down the following expression describing the extrema (maxima and minima) positions η_n (n is the extremum number) of the oscillations,

$$2\pi(t/t_{ext})_{\alpha=0}\eta_n = \zeta_n \quad (9)$$

where ζ_n are the roots of $J_0(\zeta_n) = 0$. The values of $(t/t_{ext})_{\alpha=0}$ determined for different n are close to each other (Fig. 4). The mean value of $(t/t_{ext})_{\alpha=0}$ was estimated to be $0.82 \pm 1\%$. The iron borate crystal no. 3 was also used for the temperature and field experiments described below.

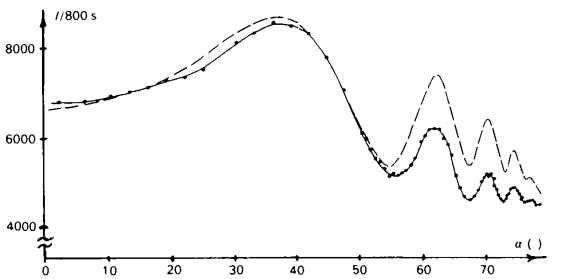

Fig. 2. Experimental (dots and solid line) and theoretical (dashed line) dependences of neutron magnetic scattering intensity on crystal inclination angle.

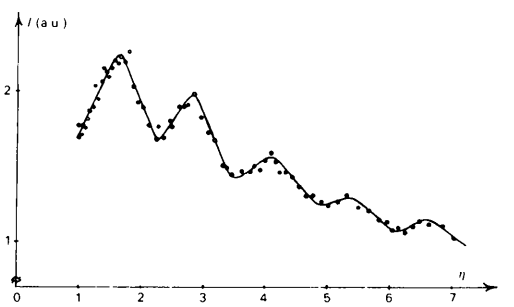

Fig. 3. Neutron magnetic scattering intensity *vs* effective optical thickness.

(2) *Temperature oscillations of intensity*

Neglecting the weak (less than 1% in the investigated temperature range) change of the Debye-Waller factor, one can write the expression for the temperature dependence of the magnetic neutron scattering intensity in the form

$$I(T) \simeq |S(T)| \int_0^u J_0(x)\,dx; \quad u = 2\pi \frac{t}{t_{ext}(T^*)} \frac{S(T)}{S(T^*)} \tag{10}$$

where T^* is room temperature.

The experiments were performed on the $FeBO_3$ crystal (Néel temperature $T_N = 348$ K) at three inclination angles, 0, 46 and 60°, corresponding to $t/t_{ext}(T^*) = 0.82$, 1.19 and 1.66 respectively. The dependence of the intensity of the coherent neutron scattering by the $FeBO_3$ crystal on temperature was measured during slow (~ 50 K h^{-1}) warming of the cryostat from liquid-nitrogen temperature up to room temperature and subsequent heating of the sample up to the Néel temperature by feeding warm air into the nitrogen container. The nondeviation of the crystal from the reflecting position with changing temperature was checked by measuring the rocking curves.

The dependence of the 100 magnetic reflection intensity on temperature oscillates. The number of oscillations rises with increasing effective crystal thickness. The temperature of approximately 348 K at which the scattering intensity goes to zero corresponds to the Néel temperature.

Fig. 5 also presents the theoretical dependences $I(T)$ calculated from (10), assuming that $S(T) \simeq B_s(T)$, where $B_s(T)$ is the Brillouin function for spin $s = \frac{5}{2}$. In the calculations we allowed for thickness inhomogeneity with (8). The correlation of scales between the theoretical and experimental curves was established by those of the absolute values of the calculated and measured integrated reflectivities at room temperature.

The nodal and antinodal positions on the experimental dependences correspond to the theoretical positions. However, the amplitude is lower than calculated. At low temperatures the magnetic scattering intensity exceeds the theoretical value for a perfect crystal. This was observed even when operating at a fixed temperature near that of liquid nitrogen and with different methods of sample mounting. To find out the reason for this excess, the temperature dependence of the nuclear neutron scattering intensity was analyzed. In this case, on cooling the crystal from room temperature down to that of liquid nitrogen, the scattering intensity increased monotonically by 35% (Fig. 6). This increase, as well as the oscillation amplitude decrease, can be attributed to the effect of elastic stresses, due apparently to the temperature gradients.

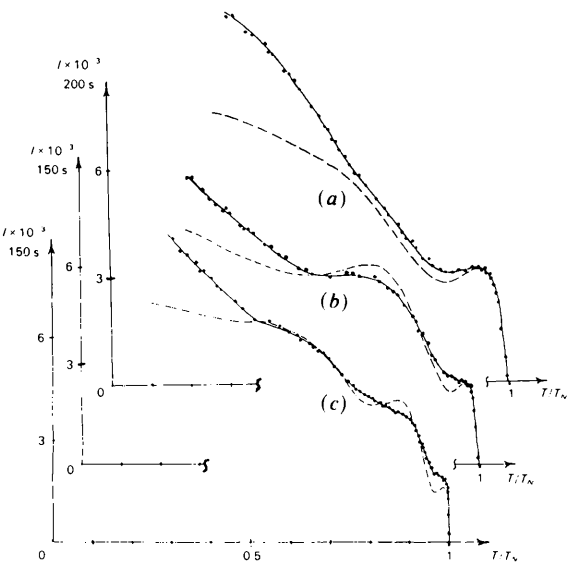

Fig. 5. Experimental (dots and solid lines) and theoretical (dashed lines) dependences of neutron magnetic scattering intensity on temperature. $t/t_{ext}(293\text{ K}) = (a)$ 0.82, (b) 1.19, (c) 1.66.

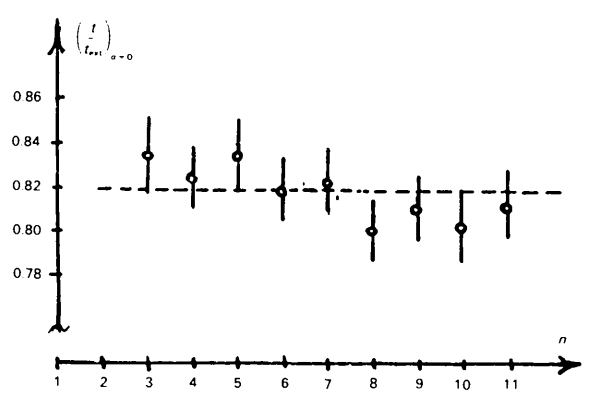

Fig. 4. The values of $(t/t_{ext})_{\alpha=0}$, calculated using (9), *vs* the extremum number.

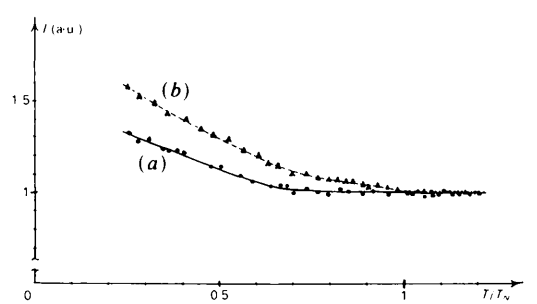

Fig. 6. The neutron nuclear scattering intensity *vs* temperature. Curve (a): crystal is placed in a magnetic field; curve (b): crystal out of the field.

Thus the intensity of magnetic neutron scattering in the perfect crystal oscillates with changing temperature in spite of the monotonic dependence of $S(T)$. These oscillations are characteristic of dynamical scattering and are absent in the case of scattering in mosaic crystals.

(3) *Intensity oscillations in magnetic-field rotation*

By using φ to denote the angle of the saturating magnetic-field rotation in the (111) plane and F_0 to denote the F value at $\varphi = 0$, we obtain the dependence of the magnetic neutron scattering structure factor on the field orientation,

$$F(\varphi) = F_0\{1 - [(\sin\varphi)(\sin\Delta)]^2\}^{-1/2}. \quad (11)$$

The expression for the scattering intensity thus takes the form

$$I[F(\varphi)] \simeq |F(\varphi)| \int_0^u J_0(x)\,dx; \quad u = \frac{2\pi t|F(\varphi)|}{t_{ext}(F_0)|F_0|}. \quad (12)$$

The experiments were carried out at room temperature at three angles of inclination: 0, 73 and 77°, corresponding to $t/t_{ext}(F_0) = 0.82$, 2.94 and 3.97 respectively. The dependence of the scattering intensity on the magnetic-field rotation angle was measured. The value of this angle was used to determine the magnitude of the magnetic scattering amplitude F.

As is seen from Fig. 7, the intensity of magnetic neutron scattering by the perfect crystal oscillates when changing the angle φ and the dependences are symmetrical with respect to $\varphi = 0$. The number of oscillations increases with rising optical thickness of the crystal. The dependences of the scattering-intensity mean value on the magnitude of $|F|$ are linear. However, these lines do not pass through the origin, which does not correspond to the results of calculations using (12). The magnitude of the 'cutoff' intensity I_0, obtained by means of extrapolation of the above-mentioned straight lines to the $|F| = 0$ value, increases with rising optical thickness of the crystal ($I_0 \simeq 0.15$ for $t/t_{ext} = 2.94$; $I_0 \simeq 0.23$ for $t/t_{ext} = 3.97$) and cannot be explained by the experimental background, the presence of neutrons of higher orders of reflection or the crystal inhomogeneity.

Apparently, this magnitude is connected with the small deviation of the crystal from an ideally perfect one, which causes the width of the deformed-crystal reflection curve to become greater than the corresponding width for an ideal crystal $\theta(F)$, by a value approximately equal to the mosaic spread σ. The peak value of the deformed-crystal curve of reflection remains at the level of the corresponding value for the ideal crystal (Klar & Rustichelli, 1973; Albertini *et al.*, 1977). Under these conditions, the integrated reflectivity is proportional to the width of the deformed-crystal curve of reflection, $R(F) \simeq [\theta(F) + \sigma]$. Since $\theta(F) \simeq |F|$, it is possible to obtain an approximate expression for the relative 'cutoff' value on the intensity axis,

$$I(F=0)/I(F_0) \simeq \sigma/[\sigma + \theta(F_0)]. \quad (13)$$

The above qualitative considerations were substantiated by numerical calculations made according to the more accurate formulae of Albertini *et al.* (1977) within the framework of an elastic mosaic-spread model. Allowance for the crystal structure defects results in the coincidence of the theoretical mean value of $I(F)$ dependences with the experimental ones. The observed 'cutoff' is described by a mosaic-spread value about 0.08″ (Fig. 7). The nodal and

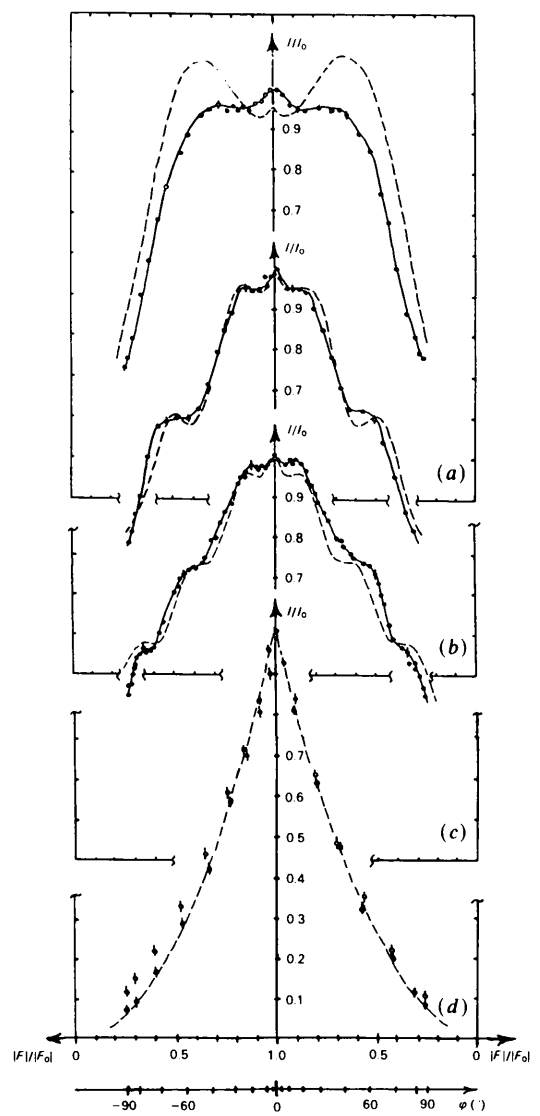

Fig. 7. Experimental (dots and solid lines) and theoretical (dashed lines) dependences of neutron magnetic scattering intensity on magnetic-field rotation angle φ and magnetic scattering amplitude F for perfect (*a*, *b*, *c*, *d*: •) and mosaic (*d*: ○) crystals. $t/t_{ext}(F_0)$ = (*a*) 0.82, (*b*) 2.94, (*c*) 3.97, (*d*: •) 0.25, (*d*: ○) 3.

antinodal positions of the theoretical and experimental dependences correspond to one another. The amplitude of oscillations on curve (*a*) is lower than the theoretical one, while the amplitudes for curves (*b*) and (*c*) are close to the calculated values. Note that it is difficult to determine a mosaic spread as small as 0.08″ from the analysis of the rocking curves.

For comparison, Fig. 7(*d*) also presents the dependences of the magnetic neutron scattering intensity on $|F|$, which was measured for a very thin ($t/t_{ext} \simeq 0.25$) perfect and a thick ($t/t_{ext} \simeq 3$) mosaic (30″) $FeBO_3$ crystal. These curves are smooth nonoscillating functions nearly proportional to $|F|^2$, as expected from kinematical theory.

(4) *Effect of magnetic defects on the amplitude of Pendellösung fringes*

Crystal defects result in a decrease of the oscillation amplitude, down to complete disappearance at large enough values of the lattice deformation. In the case of magnetic neutron scattering, the amplitude of the *Pendellösung* fringes should also be affected by the perfection of the sample's magnetic structure, which may differ from that of its crystal lattice. Let us consider the effect of a number of factors disrupting the perfection of the crystal's magnetic structure domains, magnetic orientation transition and magnetoelastic oscillations on the dynamical oscillation amplitude.

(*a*) *Effect of ferromagnetic domains.* No dynamical oscillations are observed in magnetic neutron scattering in the absence of the magnetic field (see Fig. 8). The oscillations remain in the nuclear neutron scattering, but their amplitude is reduced (Fig. 8) and the crystal reflectivity grows (Figs. 6, 8) as compared to the values measured in a saturating field. These effects can naturally be connected with the ferromagnetic domain structure (Diehl *et al.*, 1984). The domains break the spatial periodicity of the magnetic sublattice and should affect the magnetic neutron scattering due to the optical incoherence of the domains (Baruchel & Schlenker, 1989). In the case of nuclear neutron scattering, the domain structure should only be apparent due to striction deformation of the lattice, which appears (Fig. 6), as expected, only for $T < T_N$, the Néel temperature.

(*b*) *Oscillation amplitude in the vicinity of the Morin magnetic transition.* The Morin magnetic phase transition (Morin, 1950; Shull, Strauser & Wollan, 1951) from the 'easy-plane' weak ferromagnetic state to the 'easy-axis' antiferromagnetic state takes place in hematite at $T_M \simeq 253$ K. By measuring the temperature dependence of the 111 magnetic reflection intensity (whose structure factor vanishes in the 'easy-axis' state), it was established that in the investigated crystal the Morin transition occurs in the temperature range of 260–248 K.

The experiments on the dynamical oscillations were carried out in a magnetic field of approximately 4 kA m^{-1} in a cryostat. The dependence of the scattering intensity on the effective crystal thickness was studied.

The dependences of the nuclear $1\bar{1}0$ and magnetic 100 neutron scattering on the crystal effective thickness oscillate (see Fig. 9). The nodal and antinodal

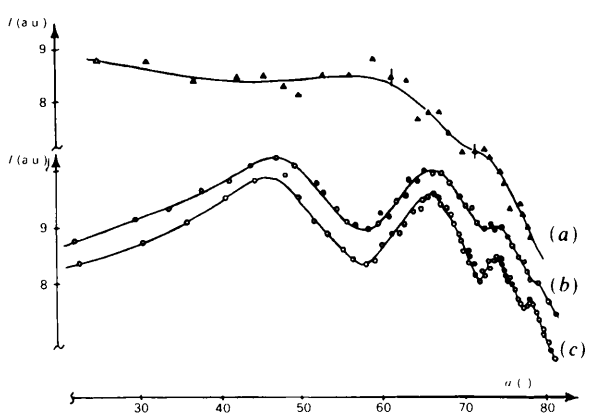

Fig. 8. Dependences of (*a*) magnetic and (*b*), (*c*) nuclear neutron scattering intensity on crystal inclination angle. Curves (*a*), (*b*): crystal is out of the field; curve (*c*): crystal is placed in magnetic field.

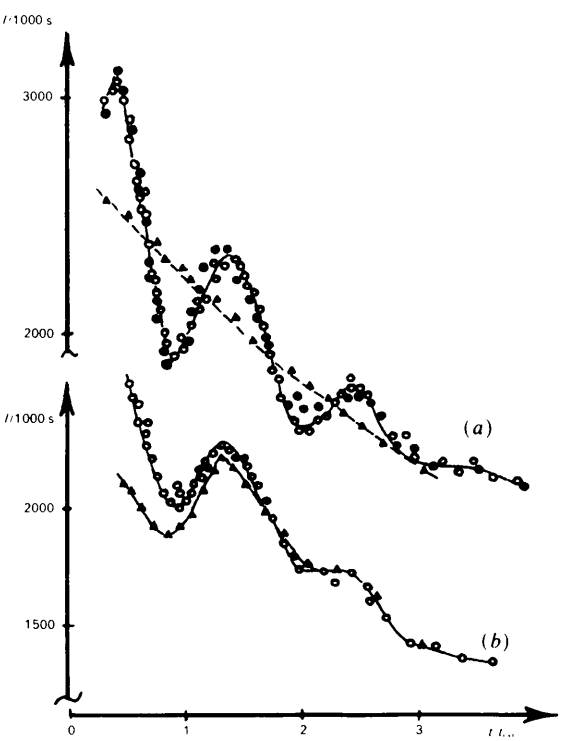

Fig. 9. Dependences of (*a*) magnetic and (*b*) nuclear neutron scattering intensity on inclination angle for a hematite crystal. The temperature was above (○), below (▲) and again above (●) the Morin transition temperature.

positions coincide with those obtained on the basis of (9). At the temperature $T \simeq 238$ K (in the antiferromagnetic phase of α-Fe_2O_3), the nuclear neutron scattering intensity remains an oscillating function of the effective thickness. The amplitudes of the oscillations and their nodal and antinodal positions are nearly the same as at room temperature. However, no oscillations are observed in magnetic neutron scattering. On heating the crystal up to room temperature, the oscillations are restored in magnetic scattering with approximately the same amplitude as before cooling.

The magnetic neutron scattering structure amplitude for the 100 reflection changes insignificantly in transition from the weak ferromagnetic phase to the antiferromagnetic one (it decreases by ~3.5%), which by itself should not cause significant changes in the diffraction pattern. The antiferromagnetic domains which interact weakly with the field may be a possible reason for the absence of oscillations in magnetic neutron scattering in α-Fe_2O_3 at $T > T_M$. The existence of these domains in hematite was also apparent in a number of other experiments (Scott & Anderson, 1965; Nathans, Pickart, Alperin & Brown, 1964).

(*c*) *Effect of magnetoelastic vibrations.* The coupled magnetoelastic vibrations represent a specific type of disturbance of the magnetic and nuclear structure of crystals. These vibrations may be resonantly excited by a relatively weak alternating magnetic field and appreciably affect the scattering intensity (Kvardakov, Somenkov & Tyugin, 1988).

The $FeBO_3$ crystal was placed in an alternating magnetic field parallel to the easy plane. The resonant frequencies were determined by the peak positions of the scattering intensity dependence on frequency. The *Pendellösung* fringe effect was investigated through the thickness dependence of the intensity of nuclear neutron scattering by the $FeBO_3$ crystal at different amplitudes of the resonant-frequency-exciting magnetic field.

It is seen from Fig. 10 that the amplitude of the *Pendellösung* oscillations vanishes with increasing field amplitude, while the scattering intensity mean value rises.

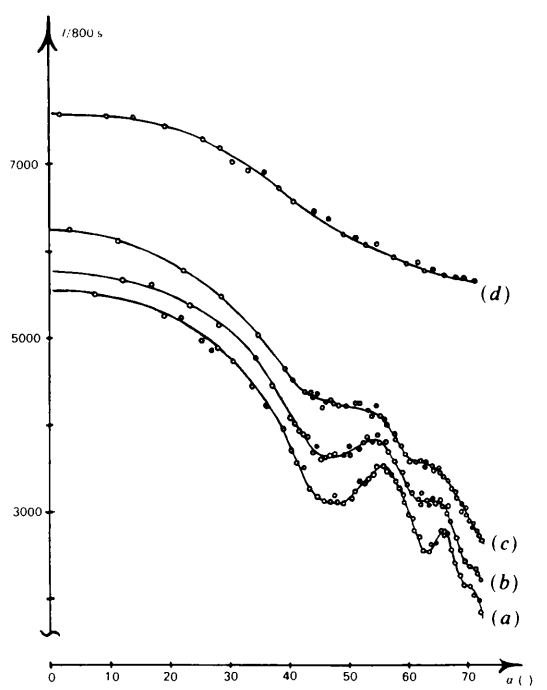

Fig. 10. Nuclear neutron scattering intensity *vs* vibrating crystal inclination angle under different amplitudes of a radio-frequency magnetic field.

Concluding remarks

The results obtained substantiate the existence of dynamical effects in magnetic neutron scattering. The positions of dynamical oscillations in the thickness dependence of intensity of magnetic neutron scattering by the $FeBO_3$ and α-Fe_2O_3 crystals are described by formulae analogous to the case of the nuclear neutron scattering.

It has been established that in a perfect crystal the magnetic neutron scattering intensity also oscillates as a function of temperature and on varying the orientation of the sublattice magnetic moments. These oscillations are due to the dynamical character of scattering and are absent in scattering by mosaic crystals. The dynamical effects in magnetic neutron scattering display the more complicated character of the interaction of neutrons with magnetic moments, as compared with the interaction with nuclei.

The amplitude of the oscillations and the behavior of the scattering intensity dependence on the structure factor allow the estimation of weak deviations from perfection of the crystalline and magnetic structure, which are difficult to detect by other methods.

The magnetic-lattice irregularities due to domain structure or a magnetic phase transition affect the dynamical effects in neutron scattering. Note that the influence on magnetic neutron scattering may be much greater (to the extent of disappearance of the oscillation) than on nuclear scattering. A radio-frequency magnetic field exciting magnetoelastic vibrations also results in *Pendellösung* oscillation suppression and scattering intensity rise.

The observed dynamical effects may be used to determine the structure factors of magnetic reflections, temperature dependences of the sublattice magnetization, form factors and spin density.

The authors would like to thank S. Sh. Shilstein, M. Schlenker and K. M. Podurets for useful discussions.

References

ALBERTINI, G., BOEUF, A., KLAR, B., LAGOMARSINO, S., MAZKEDIANU, S., MELONE, S., PULITI, P. & RUSTICHELLI, F. (1977). *Phys. Status Solidi A*, **44**, 127-136.
BARUCHEL, J., GUIGAY, J. P., MAZURE-ESPEJO, C., SCHLENKER, M. & SCHWEIZER, J. (1982). *J. Phys. (Paris)*, **43**, Suppl. No. 12, 101-106.
BARUCHEL, J. & SCHLENKER, M. (1989). *Physica (Utrecht)*, **B156**, 666-669.
BARYSHEVSKII, V. G. (1976). *Sov. Phys. Solid State*, **18**, 350-356.
BELOVA, N. E. & KABANNIK, V. A. (1985). *Kristallografiya*, **30**, 647-653.
BELYAKOV, V. A. & BOKUN, R. CH. (1975). *Sov. Phys. Solid State*, **17**, 1142-1145.
BELYAKOV, V. A. & BOKUN, R. CH. (1976). *Sov. Phys. Solid State*, **18**, 1399-1402.
DIEHL, R., JANTZ, W., NOLANG, B. I. & WETTLING, W. (1984). In *Current Topics in Material Science*, Vol. 11, edited by E. KALDIS, pp. 241-387. Amsterdam: Elsevier.
ENTIN, I. R., GLAZKOV, V. P. & MORYAKOV, V. P. (1976). *Prib. Tekh. Eksp.* **5**, 56-59.
GUIGAY, J. P. & SCHLENKER, M. (1978). *Acta Cryst.* A**34**, 229-231.
GUKASOV, A. G. & RUBAN, V. A. (1975). *Sov. Phys. Solid State*, **17**, 1972-1973.
KATO, N. & LANG, A. R. (1959). *Acta Cryst.* **12**, 787-794.
KLAR, B. & RUSTICHELLI, F. (1973). *Nuovo Cimento B*, **13**, 249-271.
KVARDAKOV, V. V., SOMENKOV, V. A. & SHILSTEIN, S. SH. (1988). *Mater. Sci. Forum*, **27/28**, 221-222.
KVARDAKOV, V. V., SOMENKOV, V. A. & TYUGIN, A. B. (1988). *JETP Lett.* **48**, 437-439.
LAUE, M. (1960). *Röntgenstrahlinterferenzen*. Frankfurt am Main: Akademische Verlagsgesellschaft.
MENDIRATTA, S. K. & BLUME, M. (1976). *Phys. Rev. B*, **74**, 144-154.
MORIN, F. J. (1950). *Phys. Rev.* **78**, 819-820.
NATHANS, R., PICKART, S. J., ALPERIN, H. A. & BROWN, P. J. (1964). *Phys. Rev. A*, **136**, 1641-1647.
SAKA, T. & KATO, N. (1986). *Acta Cryst.* A**42**, 469-478.
SCHMIDT, H. H. & DEIMEL, P. (1976). *Phys. Status Solidi B*, **73**, 87-93.
SCOTT, R. A. M. & ANDERSON, J. C. (1965). *J. Appl. Phys.* **37**, 234-237.
SHILSTEIN, S. SH. & SOMENKOV, V. A. (1975). *Sov. Phys. Crystallogr.* **20**, 670-675.
SHULL, C. G. (1968). *Phys. Rev. Lett.* **21**, 1585-1589.
SHULL, C. G., STRAUSER, W. A. & WOLLAN, E. O. (1951). *Phys. Rev.* **83**, 333-345.
SIPPEL, D., KLEINSTÜCK, K. & SCHULZE, G. E. R. (1965). *Phys. Lett.* **14**, 174-182.
SIVARDIÈRE, J. (1975). *Acta Cryst.* A**31**, 340-344.
SOMENKOV, V. A., SHILSTEIN, S. SH., BELOVA, N. E. & UTEMISOV, K. (1978). *Solid State Commun.* **25**, 593-595.
STASSIS, C. & OBERTEUFFER, J. A. (1974). *Phys. Rev. B*, **10**, 5192-5202.
UTEMISOV, K., SOMENKOVA, V. P., SOMENKOV, V. A. & SHILSTEIN, S. SH. (1980). *Sov. Phys. Crystallogr.* **25**, 845-849.
VORONKOV, S. N., PISKUNOV, D. I., CHUKHOVSKII, F. N. & MAKSIMOV, S. K. (1987). *Sov. Phys. JETP*, **65**, 624-629.
ZACHARIASEN, W. H. (1945). *Theory of X-ray Diffraction in Crystals*. New York: Wiley.
ZELEPUKHIN, M. V., KVARDAKOV, V. V., SOMENKOV, V. A. & SHILSTEIN, S. SH. (1989). *Sov. Phys. JETP*, **68**, 883-886.

Acta Cryst. (1992). A**48**, 430-442

The Structure Determination of Sindbis Virus Core Protein Using Isomorphous Replacement and Molecular Replacement Averaging Between Two Crystal Forms

BY LIANG TONG, HOK-KIN CHOI, WLADEK MINOR AND MICHAEL G. ROSSMANN*

Department of Biological Sciences, Purdue University, West Lafayette, IN 47907, *USA*

(*Received* 24 *September* 1991; *accepted* 9 *December* 1991)

Abstract

The structure of Sindbis virus core protein has been determined by a combination of multiple isomorphous replacement and molecular replacement averaging techniques. The multiple isomorphous replacement phase determinations were made for two crystal forms ($P2_1$ and $P4_32_12$) of the core protein. The real-space molecular replacement averaging was subsequently carried out between two copies of the protein per asymmetric unit in the monoclinic form and one copy in the tetragonal form. This greatly improved the quality of the electron density maps. The Sindbis virus core protein polypeptide could be traced and related to the known amino acid sequence. The averaging procedure between different crystal forms, as described in this paper, should be generally applicable to other systems.

Introduction

Sindbis virus is a small enveloped animal virus containing a single-stranded RNA genome of positive polarity. It is the type member of the alphavirus group, in the family Togaviridae. Togaviruses are known to cause a variety of diseases, such as encephalitis, fever, arthritis and rash (Shope, 1980). The nucleoprotein capsid of Sindbis virus is surrounded by a lipid membrane bilayer, through which penetrate 80 glycoprotein spikes (von Bonsdorff &

* To whom correspondence should be addressed.

0108-7673/92/040430-13$06.00